

Imaging through near-surface absorption bodies with visco-acoustic least-squares migration: a case study from the Northern Viking Graben

Thomas Latter*, Malgorzata Gregory, Andrew Ratcliffe, Graham Roberts, Bingmu Xiao, Rhea Sood and Chris Purcell, CGG

Summary

Amplitude attenuation and phase distortion of seismic data are byproducts of the Earth's anelasticity (Q). These effects are exacerbated under regions of anomalously high absorption, such as shallow gas, causing uneven image illumination and migration artifacts. We present a case study from the Northern Viking Graben in the Norwegian North Sea where we utilize single-iteration least-squares visco-acoustic prestack depth migration (Q-LSPSDM) to produce a stable Q -compensated image. The migration used high-resolution p-wave velocity and attenuation models, derived from visco-acoustic full-waveform inversion (Q-FWI). We show this workflow compensates locally for amplitude loss, eliminates the need for a Q -compensation amplitude gain limit, and enhances illumination, event coherency and AVO attributes, while reducing noise.

Introduction

Kirchhoff pre-stack depth migration (PSDM) remains the workhorse imaging algorithm in all but the most complex of geological settings. However, it suffers from migration artifacts related to the migration operator not being the inverse of the forward modeling operator (Claerbout, 1992), as well as imperfections in real-world acquisition (Huang et al., 2014). While some of these effects can be reduced by an accurate velocity model and a robust pre-processing sequence, Nemeth et al. (1999) describe least-squares migration as a way to further mitigate these issues by a least-squares solution of the inverse problem.

Xie et al. (2009) showed how absorption effects can be handled in a visco-acoustic, Q -compensating, migration (Q-PSDM) where amplitude loss and phase distortion are corrected to improve resolution. The caveat with Q -compensation is that noise gets boosted, in particular beneath shallow Q bodies where signal to noise ratios are low. This is a particular issue for the higher frequencies and an arbitrary gain limit is usually necessary, at the expense of signal recovery. Wu et al. (2017) discuss the theory of including Q in least-squares migration and Perrone et al. (2018) discuss some practical aspects of this, with the concept that Q-LSPSDM inherently favors amplification of signal over noise, hence negating the need for the arbitrary gain limit. However, there are limited studies where Q-LSPSDM has been applied to data containing anomalous, localized, spatially variable Q bodies. In this paper we demonstrate Q-LSPSDM underneath a known shallow gas

reservoir in the Norwegian North Sea using high-resolution velocity and Q models derived from Q-FWI. We show how, in comparison to Q-PSDM, Q-LSPSDM favors signal compensation over noise amplification. We also demonstrate how the improved illumination and enhanced signal to noise ratio generate improved AVO attributes.

Adding attenuation to FWI and least-squares migration

We derived our high-resolution, spatially variable, velocity and Q models from a visco-acoustic FWI scheme (Xiao et al., 2018; Xie et al., 2018, submitted to 88th Annual International Meeting, SEG). Any form of multi-parameter FWI is known to be challenging, often suffering from cross-talk between the parameters. However, for large anomalies, when using long-offset surface seismic with a non-linear inversion algorithm, there is discrimination between the amplitude and phase effects of velocity and Q (Malinowski et al., 2011). The models we have derived for this survey are discussed in Xiao et al. (2018), where both regional scale shallow Q bodies and localized gas reservoir/gas pocket accumulations are detected.

Knowing that attenuation effects are present in the real data, we can take full advantage with Q-LSPSDM. Our least-squares migration approach follows the cost effective single-iteration workflow of Guitton (2004), where the inverse Hessian is approximated by non-stationary matching filters. These filters are derived by matching a migrated/de-migrated/re-migrated image back to the initial migration and then applied to the initial migration to provide a reflectivity estimate. Curvelet-domain matching filters are utilized for this step to improve the stability and structural continuity of the process (Wang et al., 2016). Incorporating Q into the formal least-squares solution involves using visco-acoustic migrations and de-migrations at every step (Wu et al., 2017). These are more costly than their acoustic counterparts, and so we adopt a more cost effective approach described in Casasanta et al. (2017), with more acoustic and fewer visco-acoustic operations.

Northern Viking Graben (NVG) case study details

The NVG region of the Norwegian North Sea is known to contain numerous gas fields of varying size and at varying depths (e.g. Kvitebjørn or Frigg). These gas accumulations inherently exhibit attenuating properties, and hence the seismic data contain areas of amplitude loss and phase dispersion, making Q -imaging important.

Imaging through absorption with least-squares migration

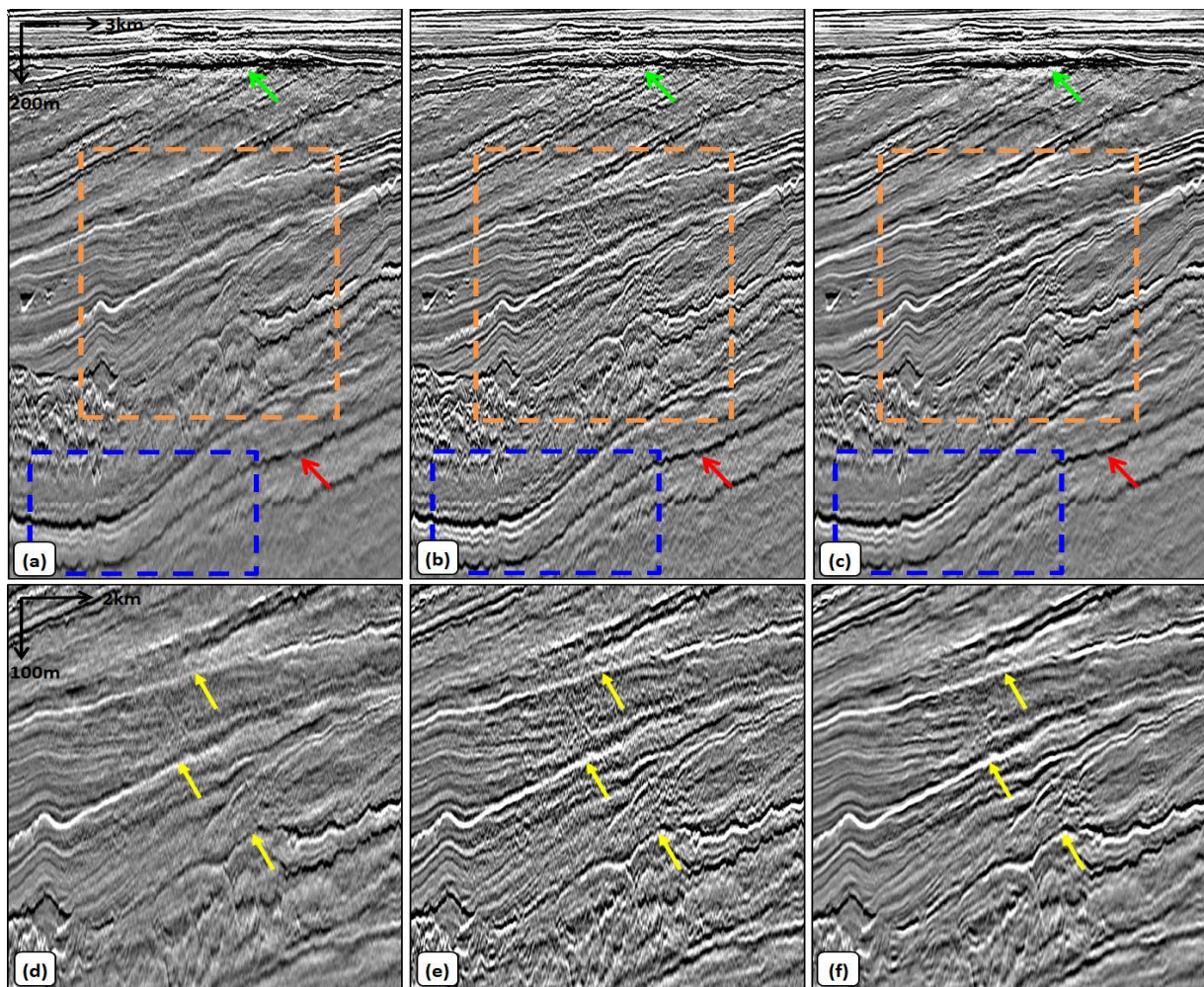


Figure 1: Stacked Kirchhoff PSDM images under the Peon gas field (indicated by the green arrows): (a) PSDM, (b) Q-PSDM with variable Q, (c) Q-LSPSDM with variable Q. Note the stable increase in resolution, enhanced structural continuity, better balanced illumination and reduced speckle and swing noise with Q-LSPSDM. (d), (e) and (f) show the corresponding zoom outlined by the orange box above. The blue box shows the area of zoom used in Figure 5, while the red arrow shows the event used for calculating the RMS amplitude maps in Figure 4.

The survey utilized variable-depth broadband streamer data acquired in 2014-2016 over nearly 36,000 km². The acquisition configuration had an 18.75 m dual source array and a sail-line separation of 450 m. There were 12 cables in total, each 75 m apart with a hydrophone group spacing of 12.5 m, and 7950 m long streamers. Pre-processing for the imaging consisted notably of a noise attenuation flow targeting swell noise, seismic interference and post critical energy, as well as broadband de-ghosting, short- and long-period free surface multiple attenuation, common offset binning and regularization. The velocity, anisotropy and Q models were derived from a sequence of tomographic inversion (Guillaume et al., 2012), Q-tomography (Hung et

al., 2008), Q-FWI (to 4 Hz) and velocity-only FWI honoring Q (to 8 Hz) using diving wave information exclusively, over the full 36,000 km² area.

Imaging the Peon gas field

The Peon gas field is a known Q body within the NVG region, situated at a depth of approximately 600 m and containing an estimated recoverable resource of 15-30 billion cubic meters of gas. We use the tilted transverse isotropic (TTI) imaging of this field to illustrate the uplift from Q-LSPSDM when applied to an area containing a localized, spatially variable Q anomaly.

Imaging through absorption with least-squares migration

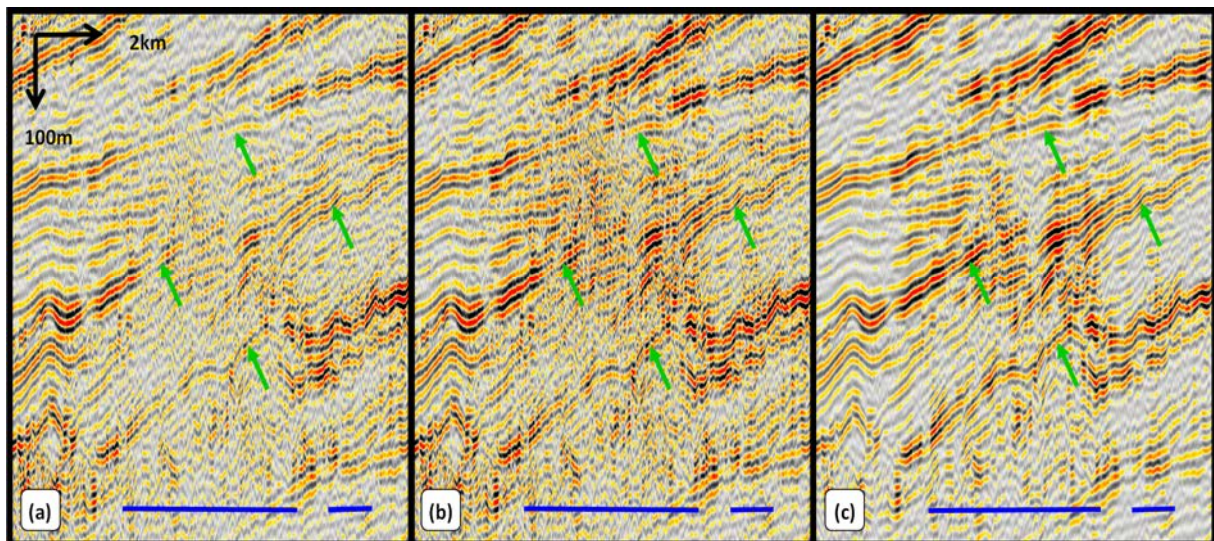


Figure 2: Stacked Kirchhoff PSDM 32-64 Hz octave panels: (a) constant $Q=200$ Q-PSDM, (b) variable Q Q-PSDM, (c) variable Q Q-LSPSDM. The blue lines denote the lateral extent of the Peon gas field. Note the laterally consistent amplitude compensation on Q-LSPSDM with minimal imprint in terms of amplitude loss or noise boosting when compared to the constant and variable Q -PSDM displays respectively (green arrows).

In Figure 1 we compare stack results of PSDM against Q-PSDM (10 dB gain limit) and Q-LSPSDM (no gain limit), where the Q model used is from high-resolution Q-FWI. In the interests of fair comparison, the +10 dB gain limit is a compromise between signal enhancement and not obviously boosting noise. The stacks of Figures 1a and 1b show the Q-PSDM flow incorporating the high-resolution Q model offers clear imaging uplift, with better focusing, structural continuity and stack response beneath the gas field, mitigating the amplitude dimming. Phase distortion is corrected and stacked events are slightly sharper, but this is not easy to see on side-by-side plots. Comparison of Figures 1e and 1f shows Q-LSPSDM gives the following uplift over Q-PSDM: 1) further improvement in event coherency (yellow arrows); 2) better lateral illumination balancing; 3) reduction in speckle noise and swing artifacts; and 4) stable Q -compensation beneath the gas body.

Amplitude analysis

Figure 2 displays the 32-64 Hz octave frequency panel of the stacks to illustrate the well-balanced event continuity and reduced noise amplification on the higher frequencies with Q-LSPSDM (Figure 2c). Note that in Figure 2a we show a Q-PSDM with a constant background Q model ($Q=200$, 10 dB gain limit), such that comparison with Figure 2b highlights the direct impact the high-resolution variable Q model has over using a background only Q model (green arrows). The lateral extent of the gas body is indicated by the blue lines. The Q-PSDM (Figure 2b) compensates the amplitudes, although it is clear from the

poorly imaged region beneath the Q body that much of this amplification is noise; hence the need for a gain limit to prevent over-boosting. A benefit of the least-squares approach is the automatic control of Q compensation, removing the gain limit necessity (Perrone et al., 2018).

Figure 3 shows a comparison of amplitude spectra extracted from the full stacks from a region beneath the gas field for PSDM, Q-PSDM (with two different dB gain limits) and Q-LSPSDM. All of the migrations containing Q show a level of amplitude compensation, but as we know from Figure 2, the Q-PSDM contains boosted noise at the higher frequencies. In contrast, the Q-LSPSDM shows an interpreted behavior of signal enhancement at the low/mid frequencies, and noise suppression at the high frequencies when compared to Figures 1 and 2 (i.e. not over-boosting noise as with the 10 dB limit Q-PSDM).

To study the imprint of the Q body in the stack volumes we compute RMS amplitude maps ± 40 ms around the deeper horizon indicated on Figure 1 by the red arrow. This is shown for the full region beneath the gas field in Figure 4. It is clear from Figures 4a and 4b that the gas field outline (white dashed line) is apparent as an amplitude dim zone in the PSDM, or constant Q Q-PSDM displays. This is partially mitigated by the variable Q Q-PSDM (Figure 4c) although the effect on signal of the arbitrary 10 dB gain limit is noticeable with slightly lower amplitudes inside the dashed lines compared to outside. It is also likely suffering from noise over-boosting (black arrows). In the Q-LSPSDM using the variable Q model (Figure 4d) the

Imaging through absorption with least-squares migration

amplitude attenuation due to the gas body appears well compensated, with minimal indication of either the shallow anomaly or amplitude over-boosting on the QC map.

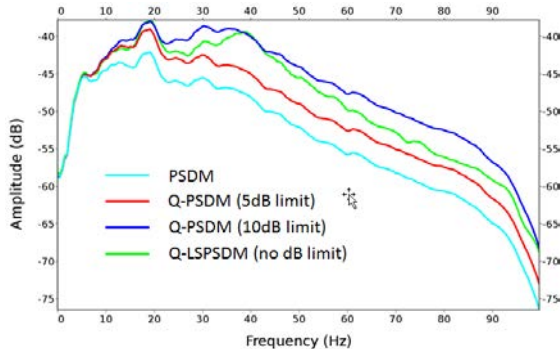


Figure 3: Amplitude spectra over 1000-2500 ms window. Note the automatic compensating effect seen with Q-LSPSDM where amplitudes are compensated without over-boosting high frequencies, compared to the arbitrarily capped Q-PSDM results.

Away from the dominant Q-body, the improvements of Q-LSPSDM can appear subtle in places, especially on stacked data. Least-squares Kirchhoff improves each common-offset image individually, making the AVO gradient a good QC of amplitude illumination and fidelity (Casasanta et al., 2017). Hence, in Figure 5 we compute AVO gradient sections from the prestack migrated gathers and compare them for a zoomed section which crosses the edge of the Q anomaly underneath the gas body. The Q-PSDM (Figure 5b) enhances signal over the PSDM (Figure 5a); however the Q-LSPSDM result (Figure 5c) is clearly favorable with better delineated structures, enhanced event continuity and reduced speckle noise everywhere, not just under the gas.

Conclusion

Using the example of the Peon gas field in the Northern Viking Graben area of the Norwegian North Sea, we have shown how a single-iteration, least-squares, visco-acoustic, Kirchhoff prestack depth migration using high-resolution FWI velocity and attenuation models gives improved imaging. This gas field is a strong localized Q-body, and the least-squares migration demonstrates more balanced illumination, improved event consistency, enhanced signal to noise ratio and improved amplitude fidelity.

Acknowledgments

We thank CGG for permission to publish this work, CGG's Multi Client and New Ventures team for permission to show the data example and Richard Higgins, Vladislav Angelov, Richard Jupp, Fred Li, Richard Wombell, and others in the Horda-Tampen processing team for support.

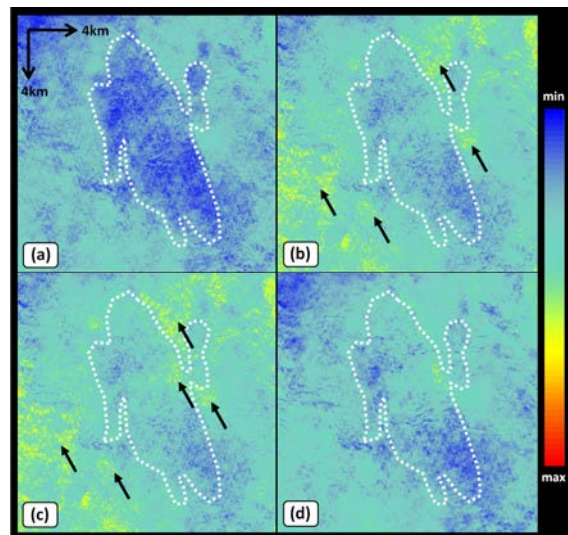


Figure 4: RMS amplitude maps computed around Top Shetland horizon: (a) PSDM, (b) constant $Q=200$ Q-PSDM, (c) variable Q Q-PSDM, (d) variable Q Q-LSPSDM. We see an improvement in amplitude consistency and noise reduction with the Q-LSPSDM.

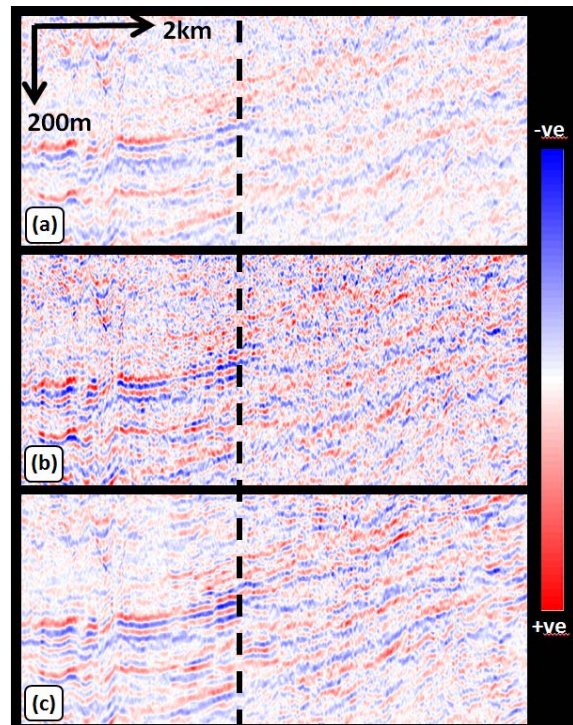


Figure 5: AVO gradient from: (a) PSDM, (b) variable Q Q-PSDM, and (c) variable Q Q-LSPSDM. The black line separates where the Q anomaly influences data to the right hand side. Note the signal continuity improvement and noise reduction on (c).

REFERENCES

- Casasanta, L., F. Perrone, G. Roberts, A. Ratcliffe, and K. Purcell, 2017, Applications of single-iteration Kirchhoff least-squares migration: 87th Annual International Meeting, SEG, Expanded Abstracts, 4432–4435, <https://doi.org/10.1190/segam2017-17704075.1>.
- Claebout, J. F., 1992, Earth soundings analysis: Processing versus inversion: Blackwell Scientific Publications.
- Guillaume, P., S. Hollingworth, X. Zhang, A. Prescott, R. Jupp, G. Lambaré, and O. Pape, 2012, Multi-layer tomography and its application for improved depth imaging: 82nd Annual International Meeting, SEG, Expanded Abstracts, 1–5, <https://doi.org/10.1190/segam2012-0683.1>.
- Guitton, A., 2004, Amplitude and kinematic corrections of migrated images for nonunitary imaging operators: Geophysics, **69**, 1017–1024, <https://doi.org/10.1190/1.1778244>.
- Huang, Y., G. Dutta, W. Dai, X. Wang, G. T. Schuster, and J. Yu, 2014, Making the most out of least-squares migration: The Leading Edge, **33**, 954–960, <https://doi.org/10.1190/tle33090954.1>.
- Hung, B., K. F. Xin, S. Birdus, and J. Sun, 2008, 3-D Tomographic Amplitude Inversion for Compensating Transmission Losses in the Overburden: 70th Annual International Conference and Exhibition, EAGE, Extended Abstracts, H004, <https://doi.org/10.1190/1.3064018>.
- Malinowski, M., S. Operto, and A. Ribodetti, 2011, High-resolution seismic attenuation imaging from wide-aperture onshore data by visco-acoustic frequency-domain full-waveform inversion: Geophysics Journal International, **186**, 1179–1204, <https://doi.org/10.1111/j.1365-246X.2011.05098.x>.
- Nemeth, T., C. Wu, and G. T. Schuster, 1999, Least-squares migration of incomplete reflection data: Geophysics, **64**, 208–221, <https://doi.org/10.1190/1.1444517>.
- Perrone, F., G. Roberts, L. Casasanta, A. Ratcliffe, A. Jafargandomi, K. Purcell, 2018, Applications of kirchhoff least-squares migration: Towards Reservoir Imaging, Adapted form extended abstract based on presentation given at the AAPG/SEG International Conference and Exhibition, Search and Discovery Article #42183
- Wang, P., A. Gomes, Z. Zhang, and M. Wang, 2016, Least-squares RTM: Reality and possibilities for subsalt imaging: 86th Annual International Meeting, SEG, Expanded Abstracts, 4204–4209, <https://doi.org/10.1190/segam2016-13867926.1>.
- Wu, X., Y. Wang, Y. Xie, J. Zhou, D. Lin, and L. Casasanta, 2017, Least square Q-Kirchhoff migration: implementation and application: 79th Annual International Conference and Exhibition, EAGE, Extended Abstracts, Tu A1 08, <https://doi.org/10.3997/2214-4609.201700804>.
- Xiao, B., A. Ratcliffe, T. Latter, X. Yie, and M. Wang, 2018, Inverting for near-surface absorption with full-waveform inversion: A case study from the North Viking Graben in the northern North Sea: 80th Annual International Conference and Exhibition, EAGE, Extended Abstracts, <https://doi.org/10.3997/2214-4609.201800681>.
- Xie, Y., S. K. Xin, J. Sun, C. Notfors, A. K. Biswal, and M. K. Balasubramaniam, 2009, 3D prestack depth migration with compensation for frequency dependent absorption and dispersion: 79th Annual International Meeting, SEG, Expanded Abstracts, 2919–2923, <https://doi.org/10.1190/1.3255457>.